SMAR 2019 – Fifth Conference on Smart Monitoring,
Assessment and Rehabilitation of Civil Structures

SMAR 2019

Restoration of structural integrity – a comparison of various repair concepts for wind turbine rotor blade shells

Carineh GHAFAFIAN [1], Bartosz POPIELA[1], Dustin NIELOW [1], Volker TRAPPE [1]
[1] Bundesanstalt für Materialforschung und -prüfung, Berlin, Germany

Contact e-mail: carineh.ghafafian@bam.de

ABSTRACT: Localized patches are a cost- and time-effective method for repairing fiber-reinforced polymer (FRP) sandwich wind turbine rotor blade shells. To increase the understanding of their effect on the fatigue of the blades, this study examines the effect of various layup methods of localized repair patches on the structural integrity of composite sandwich structures. Manufactured with the vacuum-assisted resin infusion (VARI) process, the shell test specimens are produced as a curved structure with glass fiber reinforced polymer (GFRP) sandwiching a polyvinyl chloride (PVC) foam core. Patch repairs are then introduced with varying layup techniques, and material properties are examined with cyclic fatigue tests. The transition region between patch and parent material is studied in greater detail with finite element method (FEM) simulations, with a focus on the effect of fiber orientation mismatch. Damage onset, crack development, and eventual failure are monitored with in-situ non-destructive testing methods to develop a robust understanding of the effects of repair concepts on material stiffness and strength.

1 INTRODUCTION

High-performance composite materials are increasingly used for lightweight construction due to their high specific strength and stiffness. For such applications, which include glider airplanes and wind turbine rotor blades, the materials must be able to withstand loads over an entire use lifespan, Grasse et al (2010). As more of these materials are utilized in critical parts of lightweight applications, the need for understanding the endurance of the mechanical properties and the possibilities of repairing them has become more significant, Caminero et al (2013). To-date, there exist numerous investigations on monolithic composite laminates in aircraft structural applications. However, as sandwich structures, these materials have not been studied in great depth, especially in the application of wind turbine rotor blades.

As a type of high-performance composite material, GFRPs are favored in the production of wind turbine rotor blades due to their high specific strength and stiffness properties and lower cost relative to carbon fiber reinforced polymers (CFRP), Hau (2008). During the blade manufacturing process, however, imperfections are often introduced due to a combination of numerous factors including component size, a multi-material assembly, and a large amount of manual labor. Harsh environmental conditions and a variety of loads then lead to further propagation to defects, and ultimately failure of the blade structure significantly before their designed lifespan. As replacement of entire blades can be a costly potential outcome, localized repair of the damaged shell region to restore structural integrity and thus lengthen the lifespan has become an important issue, Caminero et al (2013).

Blade shells are thus the focus of this study, produced as a composite sandwich structure with a lightweight core material between two face sheets of FRP laminate. These components are often repaired using adhesively bonded structural repair patches. These methods involve replacing the lost load path with a new material that is joined to the parent structure, and include scarf and plug patch repairs, Lekou et al (2002). The plug patch method is often utilized in rotor blade repairs done "on the ropes", as it is practical to achieve. However, scarf repairs offer a smoother load transition between patch and parent lamina. The lack of eccentricity in the load allows for low patch peel stresses, making it a highly efficient and well-suited method for repairs, especially of thick laminates due to the unlimited thickness of material that can be joined and the smooth surface produced, Lekou et al (2006). Scarf repairs are therefore often utilized on surfaces where smoothness is necessary, as they minimize potential aerodynamic disturbance, Caminero et al (2013). Figure 1a illustrates these two types of adhesively bonded repair patches.

The effects of such localized repair patches on the mechanical properties of structural components has thus become increasingly relevant for FRPs. Namely, how can the repair patches be adopted to best restore the structural integrity and thereby the lifespan of rotor blades? Impact tests as well as uniaxial tensile tests have been conducted on monolithic FRP specimens, Shufeng et al (2014), Caminero et al (2013). Hoshi et al (2007) showed an increase in residual tensile strength with decreasing scarf angle, and a study from the U.S. Department of Transportation Federal Aviation Administration showed that failure load of repaired specimens increases with decreasing scarf angle, Ahn et al (2000). A comparison of the effect of the slopes in a scarf repair on specimen strength was conducted by OPTIMAT Blades, showing a significant drop in the increase of benefit for angles less than 1:50 slope, illustrated in Figure 1b, Lekou et al (2006).

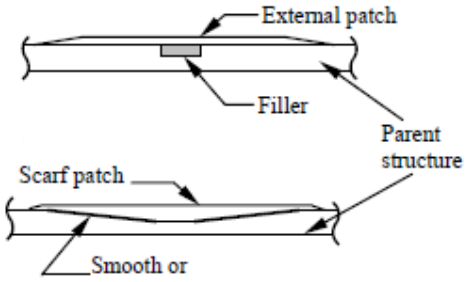

a)

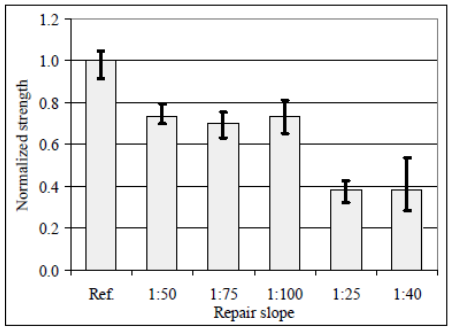

b)

Figure 1. a) Adhesively bonded repair patch methods utilized for composite structures in lightweight applications: plug patch repair (top) and scarf patch repair (bottom). b) The effect of repair patch slope on the normalized specimen strength, tested on GFRP coupons, Lekou et al (2006).

These existing studies focus on monolithic GFRP and CFRP structures. Rotor blade shell repairs as sandwich structures, on the other hand, have not been sufficiently studied to-date. In a paper by Arikan et al (2018), the behavior of GFRP sandwich plates with patch repair under three point bending tests are discussed. However, there is a lack of understanding about the effects of various repair methods on the fatigue strength and lifetime endurance of the shells of rotor blades as a curved sandwich structure, Caminero et al (2013), Trappe et al (2018).

This work therefore aims to begin to fill this knowledge gap by testing the influence of different repair patches on the structure's mechanical properties. Manufactured with the VARI process, the test specimens are produced as a curved structure with GFRP sandwiching a PVC foam core to best represent a portion of a rotor blade shell. Repair patches are then introduced with varying layup techniques and geometries, and material properties are examined with cyclic fatigue tests.

The effect of a discontinuous fiber orientation in the transition zone between repair patch and parent structure, highlighted subsequently in Figure 3, is especially brought into focus with finite element analysis (FEA) on sandwich plate specimens. The FEA simulations examine in greater detail the influence of the asymmetry caused by the patch on one side of test specimens, as well as of the fiber orientation mismatch between parent material and repair layers. Damage onset, crack development and eventual failure are monitored experimentally in-situ with non-destructive testing (NDT) methods, including thermography with an infrared camera system and a non-contact digital image correlation (DIC) based ARAMIS 3D deformation analysis system. The aim is to develop a more robust understanding of the effects of these repair concept variables on composite sandwich structures.

2 METHODOLOGY

2.1 Specimen Fabrication

The test specimens were produced as a curved sandwich structure with SAERTEX GFRP laminate face sheets and an AIREX C70.55 PVC foam core, representing a portion of a wind turbine rotor blade shell. For the biaxial (BIAX) specimens, two layers of ±45° 812 g/m^2 non-crimp glass fiber fabric were used as face sheets, whereas the triaxial (TRIAX) specimens featured an additional 0° layer with 591 g/m^2. For the clamping region, additional 1200 g/m^2 unidirectional laminate layers were used, illustrated in Figure 2. The VARI process was utilized to produce the shell specimens with the RIMR135/RIMH137 epoxy resin system from Hexion. Specimens were cured first at room temperature for 48 hours, then for 15 hours at an elevated temperature of 80°C.

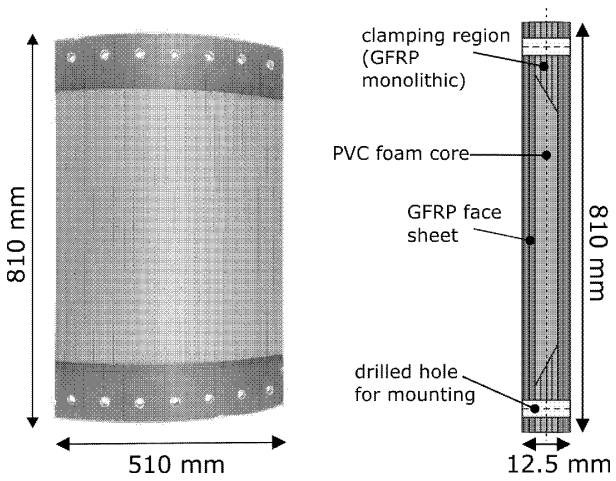

Figure 2. Sandwich test specimens designed as a representative portion of a rotor blade shell. Side view (right) shows a BIAX specimen with ±45° GFRP face sheets.

Repair patches were then applied with hand lamination onto the test specimens. The Hexion LR285/LH287 system, with a viscosity over two times as high as RIMR135/RIMH137, was used for the patches as a fast-curing epoxy resin. For replacement of the foam, a thixotropy enhancing agent was used to thicken the resin and ensure the bonding along the foam walls. Reference specimens were repaired with the plug patch as well as scarf method with a scarf slope of 1:100, while further specimens adopted a scarf slope of 1:50 based on findings from prior studies, which showed to be an agreeable compromise between mechanical property restoration and size of repair patch, Lekou et al (2006).

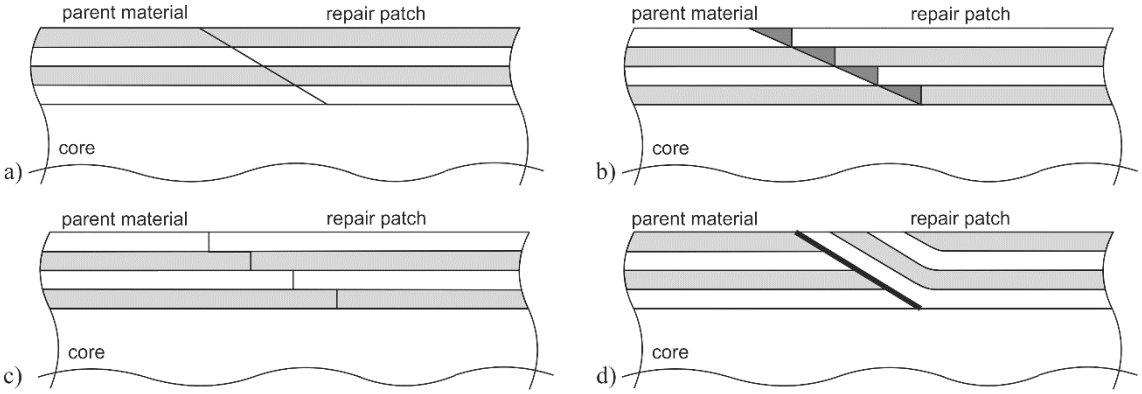

Figure 3. Scarf repair methods: a) small-to-large for two hard structures being joined (i.e. plywood), b) small-to-large with angled parent material walls, resulting in potential resin pockets in transition area (shown in dark gray), c) modified small-to-large with stepped parent walls, and d) large-to-small, with highlighted transition region of high fiber orientation mismatch. Light gray/white colors denote alternating fiber orientations (i.e. 0/90° or ±45°). Schematics represent cut out of blade shell sandwich structure, with core and repaired face sheet laminate shown.

Figure 3 schematically displays the types of scarf repair methods, with alternating fiber orientations represented by alternating light gray/white colors. Figure 3a, as the ideal fiber orientation matching scarf repair method, is only possible for two hard materials being joined, i.e. plywood. As it is impractical on the ropes to prepare repair patches in hard form, repairs are done with wet laminates onto a hard parent material. When done with the small-to-large layup arrangement, this leads to pockets of resin between the patch and parent material, as highlighted with darker gray in Figure 3b, which can decrease the stiffness and strength of the overall component. A modified scarf method with a stepped transition zone, shown in Figure 3c, is an option to the small-to-large method, but is impractical to achieve outside laboratory conditions. Thus, a large-to-small layup method, illustrated in Figure 3d, is often taken in practice as a compromise of practicality and restoration of mechanical properties. Here, however, a difference in fiber orientation in the transition region between parent material and patch thus leads to interlaminar shear stresses that could lead to early failure of the structure. A larger mismatch leads to larger stresses, Jones (1975), making this region of greater interest to study.

2.2 Mechanical and Non-destructive Testing

With the scarf method, the effect of layup structure on mechanical properties was examined. The transition region of interest, highlighted in Figure 3d, was further examined by -45°/45°/0° TRIAX test specimens with higher fiber orientation mismatch between the bottom-most repair material and the base parent material, as well as by FEM simulations of BIAX ±45° and 0/90° face sheets. The specimens were tested in a test bench integrated into a 500 kN servo-hydraulic axial machine designed at the BAM. The load of the machine is distributed between 14 hydraulic cylinders to allow for a homogeneous force application on the sample being tested.

The specimens were tested cyclically under tensile and compressive load with a stress ratio R = -1. Defect initiation and development was monitored in-situ by NDT methods including passive thermography and a DIC-based ARAMIS system for strain field measurement. Thermography functions on the principle of variations in inner features of a specimen leading to thermal contrasts at the surface when heat conduction processes are running within the bulk. Here, an ImageIR 8300 infrared camera from InfraTec was used to record the thermal contrasts. The test machine

automatically triggered the monitoring, allowing for the documentation of crack initiation and development throughout testing, shown to be an effective method for the monitoring of crack development in GFRP specimens, Müller et al (2018).

2.3 Finite Element Analysis

Utilizing the same materials and structures, an FEA of large-to-small scarf repair patches with a scarf angle of 1:50 was performed with ANSYS software on flat sandwich plate specimens. Starting with a rectangular outline, face sheet lamina walls were removed from four sides at an angle until the foam plane, creating a rectangular gradient walls geometry with four lines of intersection. SOLID186 elements with 20 nodes were utilized, corresponding to a quadratic displacement behavior in the calculations. The mesh in the repair patch region was refined by a factor of five to allow for a more complex geometry. GFRP material property values were determined in prior studies at the BAM, for the parent material in Kraus et al (2017) and for the patch material in Basan (2011). The values for the foam core were taken from the AIREX material data sheet, AIREX (2011).

3 RESULTS AND DISCUSSION

As a first step for comparison, reference shell test specimens were repaired with the plug patch method, and then with the small-to-large scarf method. Specimens were tested cyclically in tension and compression (R = -1) with a cyclic loading corresponding to outer fiber strain. The test parameters are summarized below in Table 1.

Table 1. Testing parameters of reference shell specimens under cyclic load. All specimens were tested under tensile-compression load, with a load ratio of R=-1

Specimen Name	**Repair Method**	**Test Method**	**Loading**	**Outer Fiber Strain**
BAM_SI_3_BC	plug patch	2 step fatigue	35 kN @ 3 Hz	2‰
			49 kN @ 1.5 Hz	3‰
BAM_SI_28_BC	scarf patch	fatigue	39 kN @ 1.5 Hz	3‰
BAM_SI_25_BC	scarf patch	fatigue	49 kN @ 1.5 Hz	3‰

Despite the potential for stress concentrations in edges of the plug patch repair, the specimen experienced distinctly higher damage in the regions outside the repair. ARAMIS was used to measure the strain development over a large surface of the sample. The longitudinal strain development results showed the increased local stiffness in the patch region. This led to less local deformation, especially in the specimen thickness direction. The strain field measurement also showed that the damage in the patch region begins to appear much later, only after 10^6 load cycles, and is much less pronounced than the damage outside the patch region.

3.1 Infrared Thermography Imaging

With in-situ passive thermography, the temperature distribution across the sample was followed in the region of the patch as well as around it. As depicted in Figure 4, regions of increased temperature were concentrated outside the patch for both types of repairs, following the ±45° fiber orientation. The damage within the patch appears much later and is less distinct. This points to the expected local increase in stiffness in the patch region.

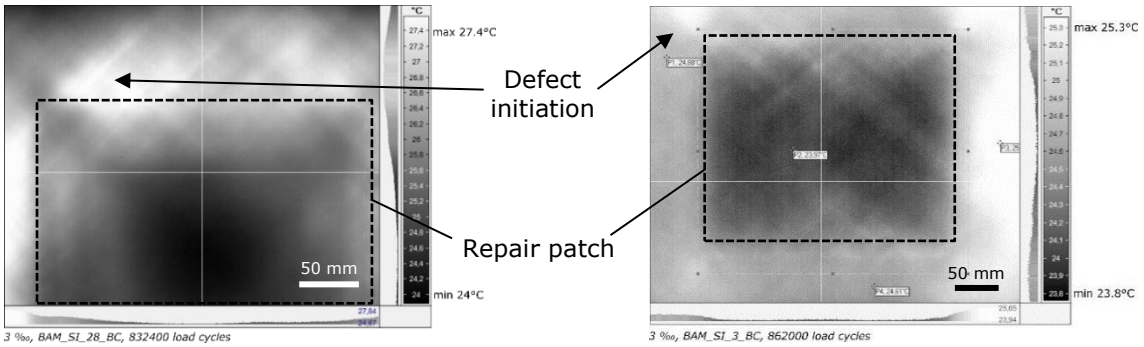

Figure 4. Experimental results - passive thermography image of scarf repaired specimen after $8.3x10^5$ load cycles (left) and plug patch repaired specimen after $8.6x10^5$ load cycles (right). The repair patch region is outlined, showing defect development and temperature increase concentration outside of this region.

3.2 Finite Element Analysis

To study in greater detail the transition region between patch and parent material for a large-to-small arrangement, sandwich plate specimens with and without repairs were compared with FEA under uniaxial tensile and compression load. Specimens were modelled with ±45° BIAX laminates as a realistic representative structure of a rotor blade shell, as well as 0/90° BIAX laminates to exaggerate the fiber orientation mismatch in the region of focus between patch and parent material. A layer-wise stress analysis was performed with a focus on the largest, bottom-most repair patch layer, where the higher fiber orientation mismatch can lead to interlaminar shear stresses, a potential source for early failure.

A deformation corresponding to 2‰ outer fiber strain was applied to the plates, based on rated wind loads experienced by rotor blades during service, Trappe (2011). The load was applied along one side, while the displacement in the load direction was hampered on the opposite side. The strain distribution resulting from the applied tensile and compressive loads varied between repaired and non-repaired samples. As seen in Figure 5, the normal strain in the direction of load (ε_x) on a non-repaired specimen does not change across the middle of the test specimen. The same region on a repaired specimen under the same load, however, showed peaks in the strain value along the edges of each repair patch layer.

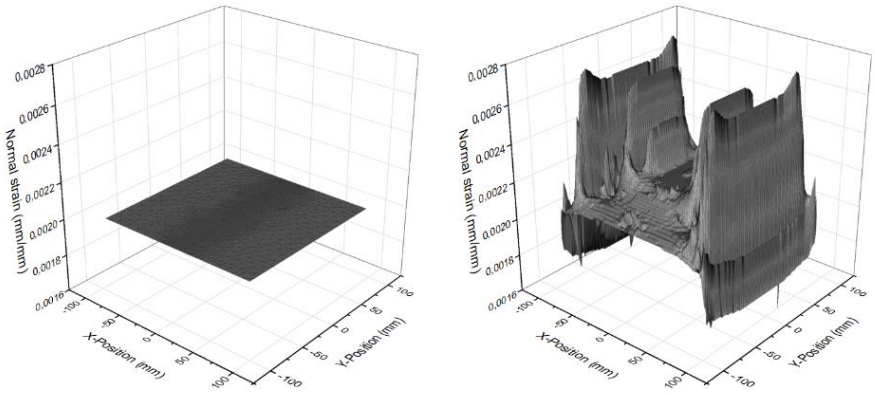

Figure 5. FEM results - strain distribution in repair patch region due to tensile load on 0/90° BIAX specimen, highlighting the difference between non-repaired (left) and repaired (right) specimens.

Furthermore, by using a calculated inverse reserve factor (IRF) to compare results of repaired and non-repaired samples, as well as compare layup types, the most critical values were observed in the transition borders between repair patch and parent material across all layers. An IRF > 1 signifies a critical value, as IRF = 1/SF, and safety factor (SF) describes the safety of a structure with respect to experienced vs designed loads. Under tensile load, the non-repaired ±45° BIAX specimen reached a maximum IRF value of 0.4154, while the repaired specimen reached the near-critical value of 0.9812. With notably higher values, the non-repaired 0/90° BIAX value maximum was 0.4781, while the specimen with repair had a maximum IRF of 1.1668, namely at the repair patch edges. Figure 6 shows these results across the repair patch field for ±45° BIAX as well as 0/90° BIAX repaired and non-repaired plates.

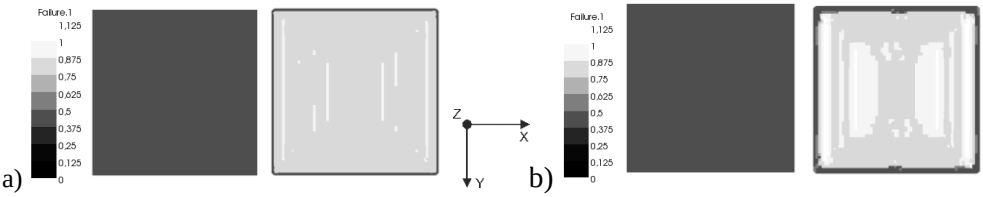

Figure 6. FEM results - comparison of IRF values under tensile load for a) ±45 BIAX and b) 0/90° BIAX non-repaired (left) and repaired (right) sandwich plates, showing critical regions along the border of each patch layer.

A layer by layer stress analysis led to the expected observation, that the highest stresses are experienced in the transition region between repair patch and parent material, namely, in the bottom-most patch layer. Additionally, in both tensile and compressive loads, stress concentrations were found along the four intersection lines of the angled patch walls, illustrated in Figure 7.

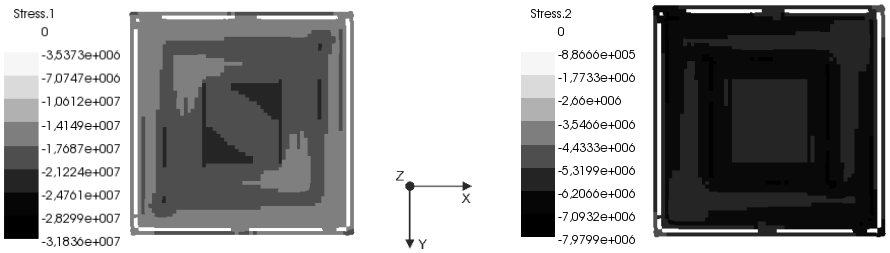

Figure 7. FEM results - stress distribution ($\sigma_{||}$ left, $\sigma_{\perp}$ right) in bottom-most repair patch layer for BIAX ±45° specimen under compressive load, units in Pa.

The stress peaks along the diagonals could be a result of the sharp corners of the intersecting walls of the rectangular repair patch, as well as the cross-linking, since the mesh in this region has not reached the ideal shape despite several refinement steps. This effect of patch geometry on stress concentrations in corners would thus be of value to investigate in future stages of this study.

4 CONCLUSIONS

The effect of local repair patches on sandwich shell specimens of rotor blades was examined. Experimental results from tensile-compressive cyclic testing of curved specimens showed greater deformation, crack initiation, as well as crack concentration outside of the patch region, caused by the local increased stiffness of the patch. Stress analysis with FEM on sandwich plates with the same material and layup structure allowed for a more in-depth focus on the transition layer between parent and patch material, proving to be the most critical layer due to the greatest

mismatch in fiber orientation. Stress concentrations in the corners of the repair patch highlighted by the FEM simulations serve as motivation to study the effect of patch geometry (i.e. elliptical vs rectangular) as a variable in the future.

5 REFERENCES

AIREX, "*AIREX® C70,"* GM--TDS-038 datasheet, Aug. 2010 [Revised Jul. 2011].

Ahn, Sung-Hoon, and George S. Springer. *Repair of Composite Laminates*. U.S. Department of Transportation Federal Aviation Administration, 2000, *Repair of Composite Laminates*.

Arıkan, Volkan, et al. "Improvement of Load Carrying Capacity of Sandwich Composites by Different Patch Repair Types." *Polymer Testing*, vol. 72, 2018, pp. 257–262., doi:.1016/j.polymertesting.2018.10.039.

Basan, Ricardo. "Untersuchung Der Intralaminaren Schubeigenschaften Von Faserverbundwerkstoffen Mit Epoxidharzmatrix Unter Berücksichtigung Nichtlinearer Effekte." *Technische Universität Berlin*, 2011.

Caminero, M.A., et al. "*Analysis of adhesively bonded repairs in composites: damage detection and prognosis.*" Composite Structures, vol. 95, 2013, pp. 500-517., doi: 10.1016/j.compstruct.2012.07.028.

Grasse, F., Trappe, V., Hickmann, S., Meister, O.: "*Lifetime assessment for GFRP-gliders using a representative substructure."* International Journal of Fatigue 32 (2010) 1, 94-99.

Hau, Erich. *Windkraftanlagen: Grundlagen, Technik, Einsatz, Wirtschaftlichkeit*. 4th ed., Springer, 2008.

Hoshi H, Nakano K and Iwahori Y. "Study on repair of CFRP laminates for aircraft structures." In: Proc 16th International Conference on Composite Materials (ICCM-16), Kyoto, July 2007.

Jones, Robert M. *Mechanics of Composite Materials*. McGraw-Hill, 1975.

Kraus, David and Volker Trappe. "Impact of Thermal Loads on the Damage Onset of Fiber Reinforced Plastics." In: Proc 21st International Conference on Composite Materials (ICCM-21), Xi'an, August 2017.

Lekou, D. J., and P. Vionis. *Report on Repair Techniques for Composite Parts of Wind Turbine Blades*. OPTIMAT Blades, 2002, pp. 1–15.

Lekou, D. J., and A. M. Van Wingerde. *Evaluation of Repair Techniques as Used for Small Specimens*. OPTIMAT Blades, 2006, pp. 1–19.

Müller, A., et al. "Investigation of the Infinite Life of Fibre-Reinforced Plastics Using X-Ray Refraction Topography for the in-Situ, Nondestructive Evaluation of Micro-Structural Degradation Processes during Cyclic Fatigue Loading." *Fatigue of Materials at Very High Numbers of Loading Cycles*, Springer Spektrum, 2018, pp. 417–439.

Shufeng, Liu, et al. "Study on Impact Performances of Scarf-Repaired Carbon Fiber Reinforced Polymer Laminates." *Journal of Reinforced Plastics and Composites*, vol. 34, no. 1, 2014, pp. 60–71.

Trappe, Volker. "Structural health monitoring for wind turbine rotor blades by strain measurement and vibration analysis." In: Proc 8th International Conference on Structural Dynamics (EURODYN 2011), Leuven, July 2011.

Trappe, Volker and Dustin Nielow. "Fatigue Loading of Sandwich Shell Test Specimens with Simulated Production Imperfections and In-situ NDT." In: Proc 7th International Conference on Fatigue of Composites (ICFC 7), Vincenza, July 2018.